Bioorganic & Medicinal Chemistry 20 (2012) 1723–1739

Contents lists available at SciVerse ScienceDirect

Bioorganic & Medicinal Chemistry

journal homepage: www.elsevier.com/locate/bmc

The effect of the length and flexibility of the side chain of basic amino acids on the binding of antimicrobial peptides to zwitterionic and anionic membrane model systems

Amanda L. Russell [a], Brittany C. Williams [a], Anne Spuches [a], David Klapper [b], Antoine H. Srouji [c], Rickey P. Hicks [a,*]

[a] Department of Chemistry, East Carolina University, Suite 300, Science and Technology Building, Greenville, NC 27858, USA
[b] Peptide Core Facility in the School of Medicine of the University of North Carolina at Chapel Hill, Chapel Hill, NC, USA
[c] Synthetic Proteomics, Carlsbad, CA, USA

ARTICLE INFO

Article history:
Received 2 November 2011
Revised 3 January 2012
Accepted 9 January 2012
Available online 18 January 2012

Keywords:
Unnatural amino acids
Antimicrobial peptides
CD spectroscopy
Isothermal Titration Calorimetry
Fluorescence spectroscopy

ABSTRACT

The intent of this investigation was to determine the effect of varying the side chain length of the basic amino acids residues on the binding of a series of antimicrobial peptides (AMPs) to zwitterionic and anionic LUVs, SUVs and micelles. These AMPs are based on the incorporation of three dipeptide units consisting of the unnatural amino acids Tic-Oic in the sequence, Ac-GF-Tic-Oic-G**X**-Tic-Oic-GF-Tic-Oic-G**X**-Tic-**XXXX**-$CONH_2$, where **X** (Spacer #2) may be one of the following amino acids, Lys, Orn, Dab, Dpr or Arg. A secondary focus of this study was to attempt to correlate the possible mechanisms of membrane binding of these AMPs to their bacterial strain potency and selectivity. These AMPs produced different CD spectra in the presence of zwitterionic DPC and anionic SDS micelles. This observation indicates that these AMPs adopt different conformations on binding to the surface of zwitterionic and anionic membrane model systems. The CD spectra of these AMPs in the presence of zwitterionic POPC and anionic 4:1 POPC/POPG LUVs and SUVs also were different, indicating that they adopt different conformations on interaction with the zwitterionic and anionic liposomes. This observation was supported by ITC and calcein leakage data that indicated that these AMPs interact via very different mechanisms with anionic and zwitterionic LUVs. The enthalpy for the binding of these AMPs to POPC directly correlates to the length of Spacer #2. The enthalpy of binding of these AMPs to 4:1 POPC/POPG, however do not correlate with the length of Spacer #2. Clear evidence exists that the AMP containing the Dpr residues (the shortest length spacer) interacts very differently with both POPC and 4:1 POPC/POPG LUVs compared to the other four compounds. Data indicates that both the hydrophobicity and the charge distribution of Spacer #2, contribute to defining antibacterial activity. These observations have major implications on the development of these analogs as potential therapeutic agents.

1. Introduction

The continued evolution of multiple-drug resistant bacteria has resulted in an intensive research effort to develop new classes of compounds that exhibit novel mechanisms of antibacterial activity.[1–7] Due to their novel mechanism(s) of action, which makes it inherently difficult for resistance to develop, natural and synthetic, antimicrobial peptides have the potential to be developed into useful antibiotic therapeutic agents.[3,5,8–11]

Our research group has previously reported the development of a series of novel AMPs incorporating unnatural amino acids into their primary sequence to impart specific three-dimensional physicochemical properties onto the peptide.[12–17] These AMPs have exhibited low μM to moderate nM in vitro MIC antibacterial activity against several strains of Gram positive, Gram negative and mycobacterium. Many also exhibited very low hemolytic activity and low acute in vivo toxicity (125 mg/kg) in mice, as well as, the ability to stimulate wound healing.[12,14]

It is well documented that the selectivity exhibited by an AMP for bacteria membranes can be correlated to the degree of complementarity of the physicochemical surface properties between the bacteria's membrane and of the interacting

Abbreviations: AMP, antimicrobial peptide; CD, circular dichroism; Dab, diaminobutionic acid; DPC, dodecylphosphocholine; Dpr, diaminopropionic acid; ITC, isothermal titration calorimetry; LUV, large unilamellar vesicles; MIC, minimum inhibitory concentration; Oic, Octahydroindolecarboxylic acid; POPC, 1-palmitoyl-2-oleoyl- *sn*-glycero-3-phosphocholine; POPG, 1-palmitoyl-2-oleoyl-*sn*-glycero-3-[phospho-*rac*-(1-glycerol)] (sodium salt); QSAR, quantitative structure–activity relationship; Tic, tetrahydroisoquinolinecarboxylic acid; SDS, sodium dodecyl sulfate; SUV, small unilamellar vesicles.

* Corresponding author. Tel.: +1 252 328 9702; fax: +1 252 328 6210.
E-mail address: hicksr@ecu.edu (R.P. Hicks).

0968-0896/$ - see front matter © 2012 Elsevier Ltd. All rights reserved.
doi:10.1016/j.bmc.2012.01.015

AMP.[4,5,7,18–21] Bacteria cells are known to contain a high percentage of negatively charged phospholipids compared to mammalian cells which contain much higher concentrations of zwitterionic phospholipids.[4,5,7,22–26] The selectivity of an AMP for a particular bacteria strain is believed to be dependent upon the chemical composition of the membrane of said bacteria. For example, the lipid bilayer of Gram negative bacteria is more complex consisting of two lipid membranes as compared to the single lipid membrane of Gram positive bacteria. Other differences between the two types of bacteria include the presence of lipopolysaccharides and porins in the membranes of Gram negative bacteria while the membranes of Gram positive bacteria are covered by a porous layer of peptidoglycan.[20,21]

The amino acid sequences of the compounds under investigation are based on the incorporation of three tetrahydroisoquinolinecarboxylic acid (Tic)–octahydroindolecarboxylic acid (Oic) dipeptide units into the polypeptide backbone separated by an amino acid spacer (Spacer #1) and by either a charged residue (Space #2) or a hydrophobic residue as shown in Figure 1. It should be pointed out that replacement of either the Tic or the Oic residue with a Gly residue dramatically alters the antibacterial activity of the parent compound.[12] Incorporation of unnatural amino acids provides us with a 'toolbox' of physicochemical properties that are not available in peptides containing only the 20 naturally occurring RNA encoded amino acids.[27–31] We have employed this 'toolbox' to facilitate the development of novel peptides with specific physicochemical properties that have the ability to interact with membranes in novel ways.[14] Thus providing a methodology for the design of bacteria strain specific AMPs.[32] The application of unnatural amino acids for the development of peptide based drugs is growing in popularity because of the inherent increased metabolic stability[10,26,29,30,33] of unnatural amino acids as compared to the 20 naturally occurring RNA encoded amino acids. This work will focus on Spacer #2 (Fig. 1), which defines the distance between the polypeptide backbone and the positively charged side chain amine group. The amino acid sequences of the peptides included in this investigation are given in Table 1. The number of carbon atoms found in the side chains for Spacer #2 are as follows: compound **4**, has a Lys residue with four carbon atoms, compound **3**, has an Orn residue with three carbon atoms, compound **2**, has a Dab residue with two carbon atoms, compound **1**, has a Dpr residue with only one carbon atom. Compound **5**, has an Arg residue with three carbon atoms, however, the amine functionality has been replaced with a guanidinium group. Spacer #2 is involved in determining the overall surface charge density of the peptide as well as defining the distance between the membrane surface and the polypeptide backbone.[12] We have previously reported that varying the number of Spacer #2 residues (Lys residues) from 3 to 5 at the C-terminus, and by relocating the Spacer #2 cluster (4 residues) to the N-terminus, the bacterial strain potency and selectivity of these analogs can be greatly improved.[14] The interactions observed for these analogs with anionic and zwitterionic LUVs and SUVs were also different.[17]

By varying the number of $-CH_2-$ groups in Spacer #2, from 1 to 4, the distance (the calculated distance is given in Table 1) between the positive charge and the peptide backbone will decrease resulting in (a) less side chain flexibility during binding; and (b) the positive charge density will reside closer to the peptide backbone. As pointed out by a reviewer, changing the number of carbon atoms in the side chain of Spacer #2, also changes the overall hydrophobicity of the residue. The combined Consensus Scale (CCS) (hydrophobicity) developed by Tossi and co-workers[34] for each residue used as Spacer #2 is given in Table 1. The net hydrophobicity resulting from the incorporation of six residues into the peptides is also given in Table 1. It is interesting to note than on this scale[34] the residue Orn found in compound **3** is the most hydrophobic of the basic residues used in this study. The chemical structures for the unnatural amino acids used in this study are given in Figure 2.

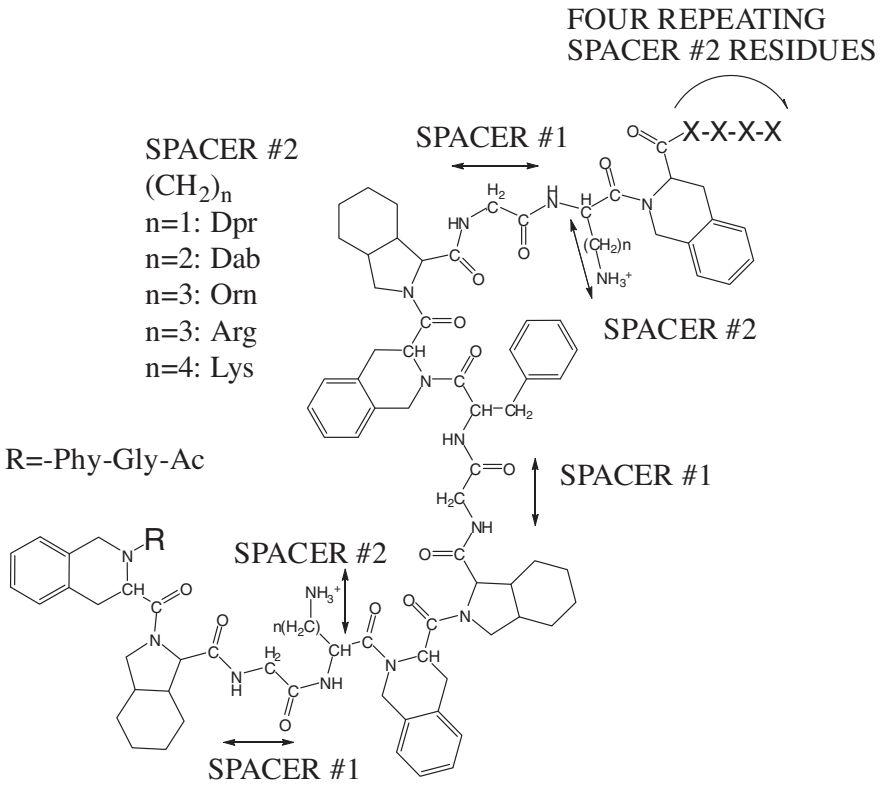

Figure 1. Basic amino acid sequence of the antimicrobial peptides used in this investigation. No secondary structure is implied by this drawing.

Table 1
Amino acid sequences for the peptides used in this investigation

Compd #	Amino acid sequence	Distance[a]	CCS[b]	CCS[c]
1	Ac-GF-Tic-Oic-G-Dpr-Tic-Oic-GF-Tic-Oic-G-Dpr-Tic-Dpr-Dpr-Dpr-Dpr-$CONH_2$	2.56	−9.3	−57.0
2	Ac-GF-Tic-Oic-G-Dab-Tic-Oic-GF-Tic-Oic-G-Dab-Tic-Dab-Dab-Dab-Dab-$CONH_2$	2.98	−9.5	−55.8
3	Ac-GF-Tic-Oic-G-Orn-Tic-Oic-GF-Tic-Oic-G-Orn-Tic-Orn-Orn-Orn-Orn-$CONH_2$	3.55	−9.0	−54
4	Ac-GF-Tic-Oic-G-Lys-Tic-Oic-GF-Tic-Oic-G-Lys-Tic-Lys-Lys-Lys-Lys-$CONH_2$	4.76	−9.9	−59.4
5	Ac-GF-Tic-Oic-G-Arg-Tic-Oic-GF-Tic-Oic-G-Arg-Tic-Arg-Arg-Arg-Arg-$CONH_2$	5.12	−10.0	−60.0

Spacer #2 is shown in Red.
[a] Average distance in angstroms from peptide backbone to the positively charged nitrogen atom as calculated using ChemDraw 3D.
[b] Combined consensus scale hydrophobicity for each charge residue.
[c] Total combined consensus scale hydrophobicity for all of the charged residues in the molecule.

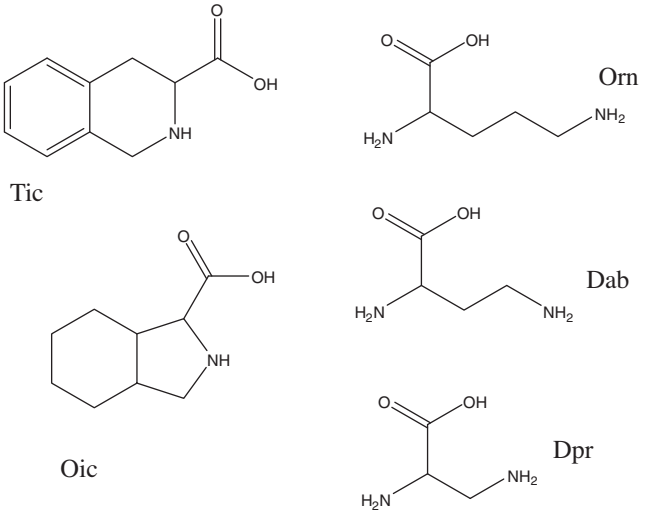

Figure 2. Chemical structures of the unnatural amino acids used in this investigation.

The in vitro antibacterial bioactivity of these peptides against selected bacteria is given in Table 2.[12,14] Compounds **4**, **3**, **2** and **5** all exhibited low in vitro μM MIC values against *Salmonella typhimurium*, *Staphylococcus aureus* ME/GM/TC resistant, *Mycobacterium ranae*, *Bacillus anthracis* AMES, *Acinetobacter baumanii* and *Acinetobacter baumanii* (drug resistant strain isolated at the Walter Reed Army Institute of Research). Compound **1** exhibited low μM MIC values against these bacteria except *M. ranae*, for which it was at least 10-fold less active than the other four analogs. Compounds **2** and **4** exhibited poor in vitro activity against *Staphylococcus aureus* (MRSA). Compound **1**, exhibited a twofold increase and compound **3**, exhibited a fourfold increase in activity against *S. aureus* (MRSA) compared to compounds **2** and **4**. Compound **5**, which contains a side chain guanidinium group (the positive charge is delocalized over two nitrogen atoms instead of only one nitrogen atom) exhibited a twofold increase in activity against *S. aureus* (MRSA) as compared to compound **4**. The flexibility of Spacer #2 appears to play a complicated role in determining the in vitro activity against *S. aureus* (MRSA). Since compounds **2** and **4** have the highest CCS values[34] (lowest hydrophobicity) and exhibited the least activity against *S. aureus* (MRSA), this suggests that hydrophobicity also plays a major role along with charge density in defining antibacterial activity against *S. aureus* (MRSA). Compound **3**, was the only analog that exhibited low μM activity against the Gram Negative strain *Yersinia pestis* and was the most active analog overall, suggesting that the Orn residue represents the optimal combination of charge density, hydrophobicity and flexibility for activity against these specific strains of bacteria. Based on this observation it appears that for this series of compounds hydrophobicity plays a dominant role in defining activity against Gram negative bacteria. The relative importance of hydrophobicity in defining activity against some strains of Gran negative bacteria was also observed with increasing the length and hydrophobicity of the amino acid residues in the Spacer #1, analogs.[14,16] As suggested by a reviewer, due to the chemical composition of the outer membranes of the other Gram negative bacteria these compounds may be unable to reach the cytoplasmic membrane and are therefore inactive. For example Gram positive strains *Staphylococcus aureus* 57% of the lipid composition is POPG, while *Staphylococcus epidermidis* 90% of the lipid composition is POPG, for *Bacillus subtilus* the percentage of POPG is reduced to 29%.[35] While the Gram negative strains *Salmonella typimurium*, *Pesudomonas cepacia* and *E. coli* contain only 33%, 18% and 6% POPG, respectively.[35]

In this investigation a combination of circular dichroism (CD) spectroscopy, isothermal titration calorimetry (ITC) and induced calcein leakage fluorescence assays were used to investigate the binding interactions of these compounds with zwitterionic and anionic micelles, LUVs and SUVs in order to develop a better understanding of how the physicochemical properties of these compounds influenced the mechanisms of lipid binding in order to design new analogs with increased therapeutic potential.

2. Materials and methods

Sodium dodecyl sulfate (SDS) and Bis–Tris buffer were purchased from Sigma–Aldrich. Monobasic and dibasic sodium phosphate, EDTA and NaCl were purchased from Fisher Scientific. 1-Palmitoyl-

Table 2
In vitro activity MIC activity (μM) against Gram Negative and drug resistant bacterial strains

Compd #	*Acinetobacter baumanii* ATCC 19606	*A. baumanii* WRAIR	*Staphylococcus aureus* ATCC 33591 (MRSA)	*Yersinia pestis* CO92	*Mycobacterium ranae* (ATCC 110)	*S. aureus* ME/GM/T (ATCC 33592)	*Brucella suis* ATCC 23445	*Bacillus anthracis* AMES	*Francisella tularensis* SCHU-S4	*Salmonella typhimurium* (ATCC 13311)	*Burkholderia pseudomallei* BURK003 (1026b)
1	3.60	3.60	114	228	100	10	228	14.80	228	3	228
2	3.40	3.40	220	220	10	10	220	6.80	220	3	220
3	6.60	6.60	53.00	26.50	10	3	106	0.82	106	3	212
4	3.2	3.2	205	205	10	3	205	12.8	100	10	205
5	5.98	24.00	96	192	10	10	192	5.98	192	10	192

2-oleoyl-*sn*-glycero-3-phosphocholine (POPC) and 1-palmitoyl-2-oleoyl-*sn*-glycero-3-[phospho-*rac*-(1-glycerol)]-Sodium Salt (POPG), and dodecylphosphocholine (DPC) were purchased from Avanti Polar Lipids. High purity calcein was purchased from Invitrogen. All chemicals were used without additional purification.

2.1. Peptide synthesis and purification

Peptide synthesis was performed either manually using *t*BOC chemistry or with an automated peptide synthesizer using FMOC chemistry[36,37] as previously reported.[12,14,15] All crude peptides were purified to 97% or greater using an AGILENT 1100 Series Preparative HPLC Instrument and a VYDAC C18 reverse phase preparative HPLC Column. All purified peptides were analyzed again by HPLC and by mass spectral analyses using a FINNIGAN LTQ ESI-MS instrument running Xcalibur 1.4SR-1 or a KRATOS PC Axima CFR Plus instrument (MALDI) running Kompact V2.4.1. ESI-MS showed multiply charged ions and the accurate mass was calculated. MALDI analyses were performed in reflectron mode as previously reported.[12,14,15]

2.2. Preparation of POPC and POPC/POPG SUVs

The appropriate amount of dry lipid was weighed out to yield a final lipid concentration of 35 μM. The lipid was dissolved in chloroform and vortexed for 3 min. The sample was dried under nitrogen for four hours and then under high vacuum overnight. The lipid was then hydrated with 2 mL of buffer (40 mM sodium phosphate, pH 6.8) and vortexed extensively. SUVs were prepared by sonification of the milky lipid suspension using a titanium tip ultrasonicator (Qsonica Sonicators model Q55) for approximately 40 min in an ice bath until the solution became transparent. The titanium debris were removed by centrifugation at 14,000 rev./min for 10 min using an Eppendorf table top centrifuge.[38] It has been reported that the mean diameter for SUVs formed by sonication is approximately 30 nm.[39,40] Final concentration used for CD studies was 1.75 mM or as otherwise stated in the text.

2.3. Preparation of POPC and POPC/POPG LUVs

A defined amount of dried POPC was weighed and suspended in buffer (40 mM sodium phosphate, pH 6.8) and spun for 30 min. For POPC/POPG (4:1 mol to mol), a defined amount of each lipid was dissolved separately in chloroform, mixed at a 4:1 ratio, then dried under a steady flow of nitrogen for 4 h and then under high vacuum overnight. The dried solutions were then hydrated in buffer and spun for 30 min. Large unilamellar vesicles (LUVs) for CD and ITC studies were prepared by extrusion using a Mini-Extruder (Avanti Polar Lipid Inc.).[41–43] The solution was passed through a 100 nm pore size polycarbonate membrane 21 times. After extrusion the LUVs were allowed to 'rest' for at least two hours before use to allow equilibration to occur. The final lipid concentration was calculated based on the weight of the dried lipid.[15,38,44–48] Kennedy and co-workers previously reported the preparation of liposomes using this procedure resulted in a homogeneous population of LUVs with >95% of the particles falling into the particle size range of 70–100 nm.[49] They also have previously shown by ^{31}P NMR that these liposomes are unilamellar.[49]

LUVs for dye release experiments were prepared as described above, but hydrated using a calcein-containing buffer (70 mM calcein, 10 mM Bis–Tris, 150 mM NaCl, 1 mM EDTA, pH 7.2, the pH was corrected using 1 mM NaOH) to give a starting lipid concentration of 35 mM. The resulting solution was vortexed for 1 min (five times). After extrusion a solution of approximately 125 μLis isolated. SEPHADEX G75 gel filtration column (eluent: buffer containing 10 mM Bis–Tris, 150 mM NaCl, 1 mM EDTA, pH 7.2) was used to remove the unencapsulated calcein from the vesicles. The fraction containing encapsulated calcein was collected (approximately 2 mL) and retained for fluorescence studies. The final lipid concentration was calculated based of the dilution of the column. The self-quenching efficiency (Q) for each lipid solution was calculated using the following equation: $Q = [1 - (F_0/F_T)] \times 100\%$ where F_0 and F_T are the background fluorescence before treatment with peptide and after treatment with of 10% Triton X, respectively. The minimum Q value used was 80%.[15,38,45–48,50–53]

2.4. Circular dichroism

For buffer studies 200 μM peptide concentrations (40 mM phosphate buffer, pH 6.8) were used. Binding studies were conducted using peptide concentrations of 100 μM for compounds **3**, **2** and **5** and 200 μM for compounds **4** and **1** in the presence of 1.75 mM POPC LUVs or at a concentration of 200 μM for compounds **4**, **3**, **1** and **2** and 100 μM for compound **5** in the presence of 1.75 mM 4:1 POPC:POPG LUVs in 40 mM phosphate buffer (pH 6.8). For the binding studies using SUVs peptide concentrations of 100 μM were used in the presence of 1.75 mM POPC SUVs or in the presence of 1.75 mM 4:1 POPC/POPG SUVs in 40 mM phosphate buffer (pH 6.8). For micelle studies peptide concentrations of 100 μM in the presence of 80 mM micelles in 40 mM phosphate buffer (pH 6.8) were used. All CD spectra were obtained on a JASCO J-815 CD Spectrometer using a 0.1 mm cylindrical quartz cell (STARNA CELLS, Atascadero, CA) at room temperature. Each spectrum (260 to 190 nm) was the result of the average of 8 scans with a scanning speed of 20 nm/min, a 1 nm bandwidth, a data pitch of 0.2 nm, a response time of 2.0 s and sensitivity of 5 mdeg. All spectra were baseline corrected by subtracting the lipid spectra to eliminate contributions due to LUVs or SUVs. All analysis of CD spectra was conducted after smoothing (means-movement with convolution width of 5–25) and conversion to molar ellipticity using the JASCO Spectra Analysis program.[41,54]CD spectra that exhibit HT values of greater than 400 were not used due to excessive light scattering or adsorption of light.

2.5. Isothermal titration calorimetry

Data was acquired using a MICROCAL VP-ITC calorimeter (Northampton, MA). All experiments were run in 40 mM sodium phosphate buffer, pH 6.8, at 25 °C. All solutions were degassed for approximately 10 min under vacuum before loading the reaction cell and syringe. For full titration experiments, 15 μL aliquots of 35 mM LUVs solutions in buffer were titrated into peptide (100–200 μM). For binding single injection experiments, 15 μL of dilute samples of peptide (100–200 μM) were titrated into excess LUVs (15–20 mM). A stirring speed of 220 rpm and injection duration of 30 s were chosen to ensure sufficient mixing while keeping the baseline noise to a minimum. To ensure complete equilibration, a delay of 700 s between injections was used. The background heat of dilution was obtained by titrating LUVs into the reaction cell containing only buffer and was subtracted prior to analysis. Data was analyzed with Origin® software (version 7.0). ITC data collection was obtained in duplicate in an effort to ensure reproducibility.[15,38,41,45–48,55]

There are two different models to consider when analyzing thermodynamic data obtained from ITC thermograms. The first and simpler model, does not take into account the electrostatic interactions between the peptide and membrane surface while the second considers these interactions.[46] The former model, and simplest of the two, involves the partitioning of the peptide between the aqueous phase and the lipid membrane, assuming equation 1 as determined by Wieprecht and Seelig[46] is a linear relationship:

$$X_b = K_p c_f \quad (1)$$

X_b is the molar ratio of membrane-bound peptide per lipid, c_f is the concentration of free peptide in solution and K_p is the partition coefficient.

The second model takes into consideration electrostatic interactions between the peptide and lipid surface. Given that the peptides under investigation are highly positively charged and the LUVs surface contains regions of positive and negative charge, the second model is the more relevant for our analysis. The membrane surface contains localized regions of negative charge which will attract the positively charged residues of the AMP to the surface of the LUV. This results in an increase of AMP concentration at the surface of the membrane, c_m in comparison to the bulk solution, c_f.[56] Therefore, Eq. 2[46,57–59] is more appropriate for the analysis of this data.

$$X_b = K c_m \quad (2)$$

By plotting X_b versus c_m, K can finally be obtained as the slope.[46,57–59]

Knowing K allows for the calculation of other thermodynamic data, including free energy (ΔG) and entropy (ΔS) from the following Eqs. 3 and 4.[46,57–59]

$$\Delta G^0 = -RT \ln 55.5K \quad (3)$$

$$\Delta G^0 = H - \Delta TS \quad (4)$$

2.6. Calcein leakage assays

Peptide induced calcein leakage studies were conducted using an ISS PC1 photon counting spectrofluorometer (ILC Technology) at an excitation wavelength of 494 nm and an emission wavelength of 518 nm. An aliquot of peptide (4–20 μM) in buffer (10 mM Bis–Tris, 150 mM NaCl, 1 mM EDTA, pH 7.2) was added to the cell containing calcein-encapsulated liposomes (36.6 μM lipid concentration). Measurements were taken every minute for the first 20 min of the experiment and every 10 min after until no further changes in the emission intensity occurred (approximately 90 min). To determine the maximum fluorescence intensity that corresponds to hundred percent leakage, an aliquot of 10 μL of a 10% Triton X solution was added to the sample at the end of each experiment. The apparent percent leakage was calculated using the following equation: % leakage = $[1 - (F_0/F_T)] \times 100\%$, where F_0 and F_T are the initial fluorescence before introduction of peptide and after the addition of Triton X, respectively.[15,51,52] Prior to use, each batch of calcein encapsulated liposomes were subjected to a self-quenching efficiency test. The self-quenching efficiency (Q) for each lipid suspension was set at a minimum value of 80% before it could be used in these investigations. The Q value was calculated using the following equation: $Q = (1-(F_0/F_T)) \times 100\%$ where F_0 and F_T are the background fluorescence of the lipid suspension and the total fluorescence after the addition of Triton X, respectively.[53,60–62]

3. Results and discussion

The study of Spacer #2 focuses on the affect the length of the positively charged side chain has on the interaction of these compounds with membrane model systems of varying chemical composition. Shortening the side chain of the charged residue decreases the distance between the peptide backbone and the positively charged amine. This will affect the distribution of the electrostatic surface potential and bring it closer to the backbone of the peptide. Also, by decreasing the number of methylene groups in the side-chain, the degree of molecular flexibility available to allow for reorienting the peptide backbone and the charged side chains relative to the membrane surface is reduced. In addition changing the number of carbon atoms in the side chain of Spacer #2, will also change the resulting hydrophobicity of the side chain. This change will result in changing the overall hydrophobicity of the peptide. In order to determine the effects of Spacer #2 on the binding interactions with bacterial and mammalian membranes, large unilamellar vesicles (LUVs) and small unilamellar vesicles (SUVs) consisting of 1-palmitoyl-2-oleoyl-*sn*-glycero-3-phosphocholine (POPC) were selected as simple models for the zwitterionic membranes of mammalian cells. LUVs and SUVs consisting of (4:1) 1-palmitoyl-2-oleoyl-*sn*-glycero-3-phosphocholine (POPC)/**1-**palmitoyl-2-oleoyl-*sn*-glycero-3-[phospho-*rac*-(1-glycerol)] (Sodium Salt)) (POPG) were selected as simple models for the anionic membranes of bacteria membranes. These models were used to investigate the interaction associated with the inserted state process of membrane binding.[54] The selection of mixed POPC/POPG lipids was not the best choice to mimic the lipid composition of bacteria membranes since POPC is normally not found in the membranes of bacteria. However, it was selected to allow for comparison of our results to previously reported investigations of peptide lipid interactions.[44,45,47,58,62–64] LUVs were selected instead of SUVs for ITC and induced calcein leakage studies because they are considered to more closely resemble biological membranes since LUVs are not subject to the increased curvature stress associated with SUVs.[38,40,65,66] In addition, in this investigation we will use anionic and zwitterionic micelles to isolate and investigate the surface binding interactions of these peptides from the aggregation and pore forming interactions that occur on binding to liposomes.

3.1. Calcein leakage studies

The first step in this investigation was to determine how Spacer #2 affects membrane disruption. The monitoring of the fluorescence of calcein by peptide induced leakage from LUVs, is a well-documented technique to confirm membrane disruption by AMPs.[64,67] Different concentrations of AMPs (4–20 μM) were introduced to solutions of either POPC (Fig. 3) or 4:1 POPC/POPG LUVs (Fig. 4) and the resulting induced fluorescence due to leakage of calcein was monitored over a 90 min time period.

As the length of Spacer #2 decreases, the percentage of induced calcien leakage from POPC LUVs increases, at a AMP concentration of 20 μM the induced leakage increases from approximately 25% for compound **4** to approximately 100% for compound **1**. The observed increase in induced calcein leakage from POPC LUVs is consistent with the observed ITC data which indicated an increase in binding to POPC LUVs with decreased Spacer #2 length. The induced calcein leakage for each individual AMP also increased over a narrow range as a function of increasing peptide concentration. At concentrations of both 4 and 20 μM compound **5** induced approximately 60% calcein leakage. Compound **5** was the only AMP where the induced calcein leakage did not vary with peptide concentration. This data suggests that charge delocalization found in compound **5** (Spacer #2 is an Arg residue) causes it to interact with POPC LUVs in a different way than with the other four compounds. There appears to be no correlation between the hydrophobicity of Spacer #2 and the induced calcien leakage from POPC LUVs. This data would suggest that these compounds would exhibit high hemolytic activity, which is a concern that may limit the use of these of analogs to topical administration. Members of this class of AMPs have been shown to stimulate wound healing in un-infected wounds.[12] However, we have previously reported that several analogs with high hemolytic activity exhibited no toxic effects in a mouse maximum tolerated dose study at dosages of 25 mg/kg[12] while exhibiting efficacy in vivo against bacterial

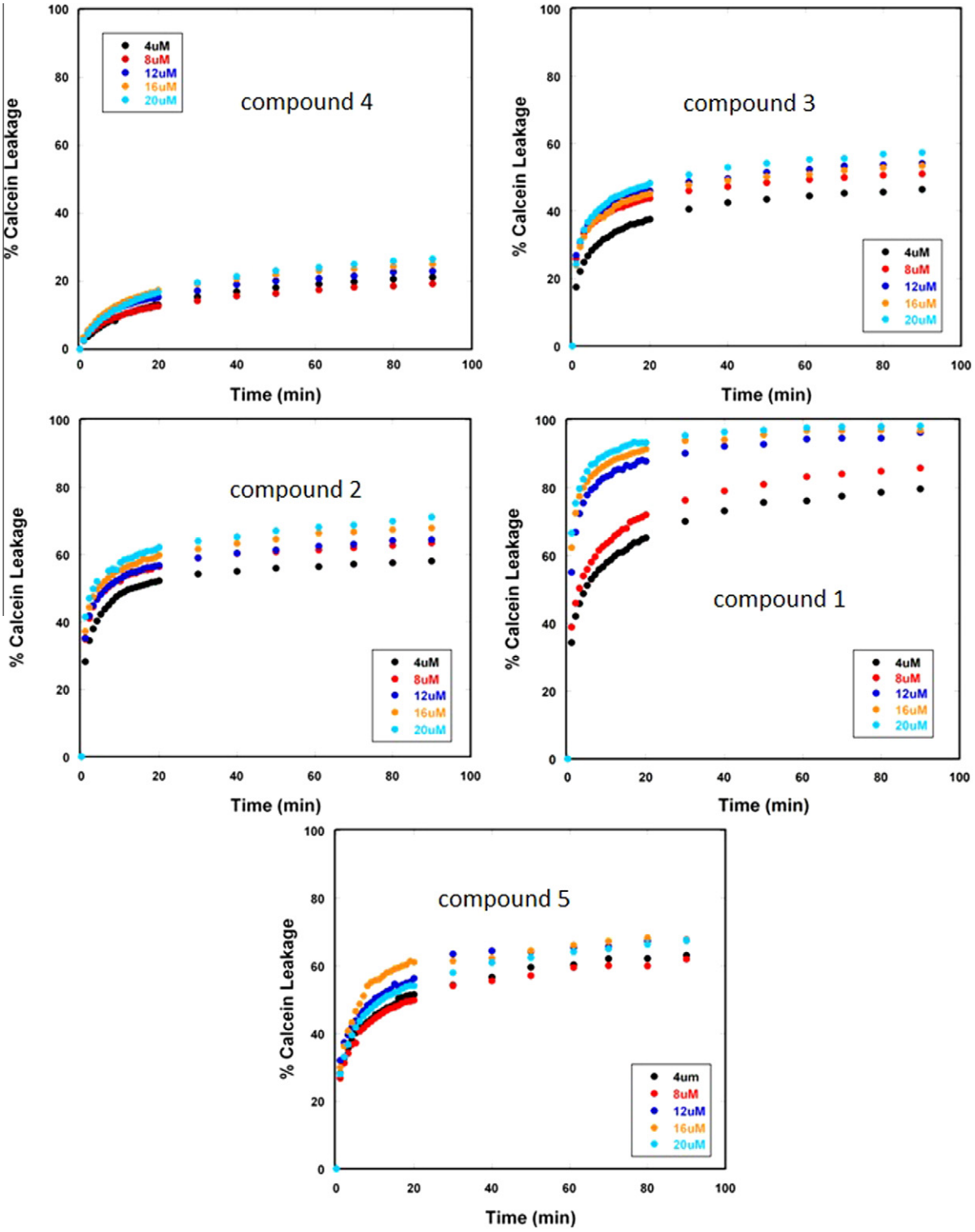

Figure 3. The time dependent release of calcein from POPC LUVs induced by increasing concentrations of compounds **4** (top left), **3** (top right), **2** (middle left), **1** (middle right) and **5** (bottom) as measured by fluorescence.[52,50,41]

infections at a dose of 5 mg/kg for as long as 20 days of administration (unpublished results).

As the length of Spacer #2 decreases the percentage of induced calcien leakage from 4:1 POPC/POPG LUVs increases. At a peptide concentration of 20 μM the induced leakage increases from approximately 40% for compound **4** to approximately 100% for compound **1**. The induced calcein leakage for each individual AMP also increased over a much wider range as compared to that observed with POPC LUVs as a function of increasing peptide concentration. Unlike the concentration independent behavior observed for compound **5** in the presence of POPC LUVs, at a concentration of 20 μM compound **5** induced approximately 90% calcein leakage and at a concentration of 4 μM compound **5** induced only approximately 50% leakage. Based on this observation the delocalization of positive charge found in compound **5** does not play as large a role in the interaction with 4:1 POPC/POPG LUVs

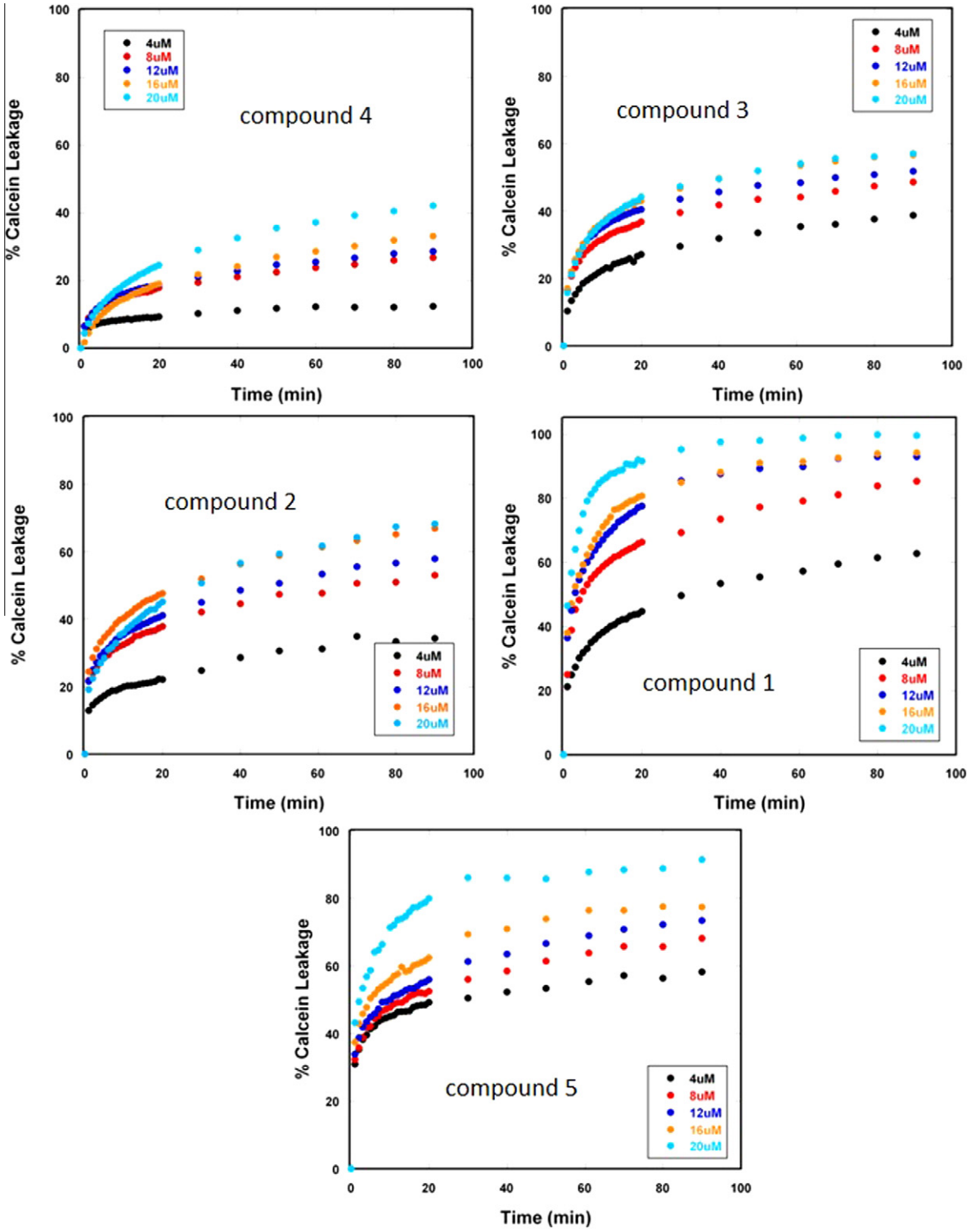

Figure 4. The time dependent release of calcein from 4:1 POPC/POPG LUVs induced by increasing concentrations of compounds **4** (top left), **3** (top right), **2** (middle left), **1** (middle right) and **5** (bottom) as measured by fluorescence

as it does with the interaction with POPC LUVs. Once again no correlation between the hydrophobicity of Spacer #2 and the induced leakage from 4:1 POPC/POPG LUVs exists.

The calcien leakage data suggest that these peptides interact with POPC and 4:1 POPC/POPG LUVs via different mechanisms. However, none of these peptides exhibited any selectivity for one liposome over the other.

3.2. CD spectroscopy

The application of CD spectroscopy to monitor conformational changes of peptides and proteins in various environments is well documented and widely employed due to its high sensitivity.[40,68,69] Traditionally SUVs have been employed almost exclusively in CD spectroscopy to investigate the binding of peptides

and proteins with lipids in order to minimize the contribution of light scattering on the spectra.[39,40] However, the work of Ladokhin and co-workers have shown that undistorted CD studies can be obtained in the presence of up to 3 mM LUVs above 200 nm and in the presence of 7 mM LUVs above 215 nm.[40] In this study we are employing both SUVs and LUVs to investigate the binding interactions that occur between these AMPs and either zwitterionic or anionic liposomes to determine the effect of membrane curvature on binding. In addition, anionic and zwitterionic micelles will be used to isolate and investigate the surface binding interaction of these peptides from the aggregation and pore forming interactions that occur on binding to lipids.

In the analysis of CD data it must be noted that the CD spectrum of a peptide represents the linear combination of a number of different conformers.[68,70] This is particularly true when liposomes are used as there are many different peptide–liposome interactions possible depending on the peptide to lipid ratio and on the type of lipid present. Changes in the intensity or shape of the CD spectrum of a peptide in the presence of a liposome indicate that the peptide is adopting different conformations on interacting with that particular liposome as compared to another environment such as a buffer.[68,70] Due to the high percentage of unnatural amino acids incorporated into the peptide under investigation here, no quantitative estimation of secondary structural features is possible.

3.2.1. Micelle studies

Micelles are excellent models to study the surface interactions that occur between peptides and membranes. Micelles do not form bilayers and therefore peptides are unable to fully insert into micelle to form pores as is the case with phospholipids. For this investigation DPC micelles[53] were selected as a simple model for zwitterionic lipids of eukaryotic cells and SDS micelles[71] were selected as a simple model for anionic lipids of prokaryotic cells. The CD spectra of compounds **4** (Lys), **3** (Orn), **2** (Dab), and **5** (Arg), in 40 mM phosphate buffer (pH 6.8) (Fig. 5A) are all very similar in shape. However, the spectral intensities vary in a random fashion and do not correlate with the length of Spacer #2. In the presence of negatively charged micelles (SDS), the CD spectra of compounds **4**, **3**, **2**, **1** and **5** (Fig. 5B) are very similar in shape and intensity to each other. The CD spectra of compound **1** (Dpr) with the shortest Spacer #2, appears to exhibit a slight change in shape around 200 nm, suggesting slightly different binding interactions with SDS micelles than that observed for the other four compounds. There is no apparent correlation between the intensities of the λ_{min} at approximately 200 nm and the length of Spacer #2. However, the intensities of λ_{max} at approximately 190 nm correlate with increasing Spacer #2, length for compound **4**–**1. As** seen in Figure 5C, in the presence of zwitterionic DPC micelles, the shape and intensities of the CD spectra are somewhat different from the spectra observed in the presence of SDS micelles. The most striking difference between the CD spectra in the presence of SDS and DPC is the spectra of compound **2**. In the presence of SDS micelles the CD spectrum of compound **2** is the least intense of the five compounds, however in the presence of DPC the CD spectrum of compound **2** is the most intense of the five CD spectra. No correlation between Spacer 2, or either the λ_{max} or the λ_{min} of these peptides was observed.

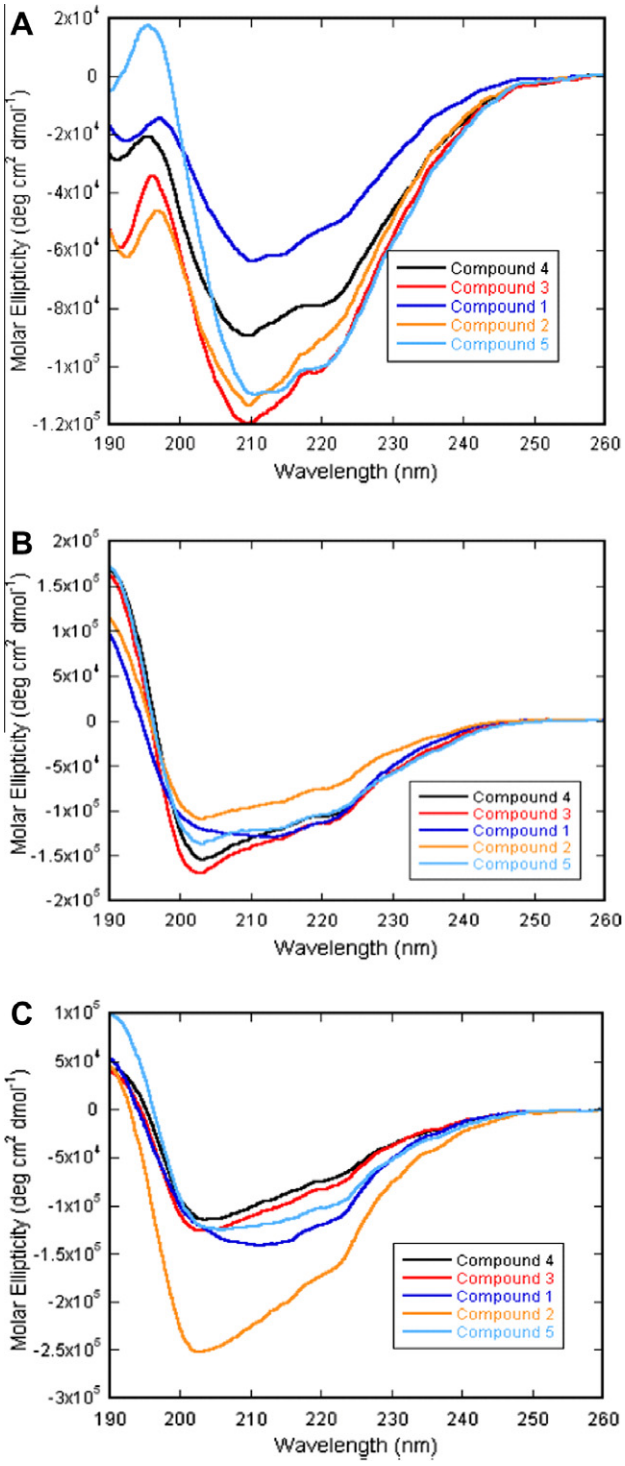

Figure 5. Far-UV circular dichroism spectra of compounds **4**, **3**, **2**, **1** and **5** in the presence of (A) 40 mM phosphate buffer, pH 6.8; (B) 80 mM SDS in 40 mM phosphate buffer, pH 6.8; (C) 80 mM DPC in 40 mM phosphate buffer, pH 6.8.

3.2.2. POPC LUVs

The CD spectra of compounds **4**, **3**, **2**, **1** and **5** in the presence of 1.75 mM POPC LUVs are given in Figure 6A. The CD spectra of these compounds exhibited changes in intensity and or shape, and all experienced shifts in λ_{max} and λ_{min} in the presence of POPC LUVs as compared to their respective spectra in buffer (Fig. 5A) and DPC micelles (Fig. 5C). The CD spectra obtained in the presence of DPC micelles clearly indicate that these compounds are adopting different conformations compared to the conformations adopted in the presence of POPC LUVs, suggesting that the surface bound and the lipid inserted conformations are different, as expected. The CD spectra of compound **5** which contains a guanidinium side chain, where the positive charge is delocalized over two nitrogen atoms instead of being localized on one nitrogen atom as is the case for the other four compounds (with amine functionality), also adopts a different and unique conformation(s) on binding to POPC LUVs.

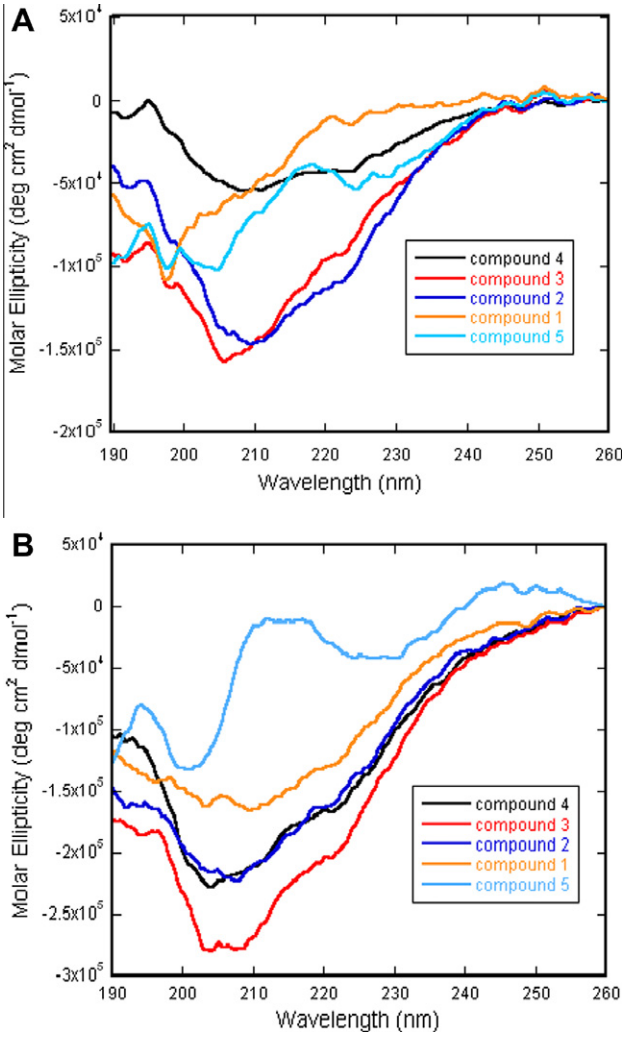

Figure 6. Far-UV circular dichroism spectra of 100 μM solutions of compounds **4**, **3**, **2**, **1** and **5** in the presence of (A) 1.75 mM POPC LUVs; (B) 1.75 mM POPC SUVs.

This data is direct experimental confirmation that by decreasing the length of Spacer #2 the distance between the positive charge and the peptide backbone will result in (a) less side chain flexibility during binding, (b) the positive charge density will reside closer to the peptide backbone and (c) changes in the hydrophobicity of the molecule and thus will affect the conformations adopted by these compounds on binding to LUVs.

Pseudo titrations of the AMPs with POPC LUVs are given in Figure 7 for compounds **4**, **3**, **2**, **1** and **5**. Peptide concentrations of 100 μM for compounds **2**, **3** and **5** and concentrations of 200 μM for compounds **4** and **1** were used with POPC concentrations varying from 0.8 to 12 mM. As can be seen from the CD spectra for each compound, the intensity of the spectra vary but the general shape of the spectra are similar. As expected based on the work of Ladokhin and co-workers[40] the spectra at higher POPC concentrations are distorted (i.e., increased noise) at the lower wavelengths. However, even at the highest POPC concentrations, the observed CD spectra are very similar above 200 nm. This data suggests that no major changes in peptide conformation(s) are occurring with increased POPC concentration.[72,73]

3.2.3. POPC SUVs

Comparing Figure 6A with B it appears that CD spectra obtained in the presence of POPC SUVs and LUVs are dissimilar. As pointed out by Ladokhin and co-workers,[40] differences in the CD spectra of membrane associating peptides bound to SUVs and LUVs are to be expected. The comparison of these spectra are complicated by various factors including; (1) Differences in the curvature and other structural features including lipid packing density of the SUVs compared to the LUVs that may affect the conformation(s) adopted by the bound peptide,[40,74,75] (2) Differences in the binding affinity of the peptide for SUVs compared to LUVs are possible. SUVs are known to exists as non-equilibrium systems that produce artificially high binding affinity,[74] and (3) The light scattering of LUVs at high lipid concentrations can also distort the CD spectrum.[74] Both Huang and co-workers[75] and Ladokhin and co-workers[40] reported that the appearance of the CD spectra of SUV and LUV bound peptides maybe different. Clearly on binding of these AMPs to POPC SUVs there is no correlation to the λ_{min} at approximately 205 nm with the length of Spacer #2. The differences in the CD spectra for these AMPs bound to POPC LUVs and SUVs are further illustrated in Figure 8. For compound **4** the CD spectrum in POPC SUVs exhibits the same shape however it is much more intense than the CD spectrum observed in LUVs. This data suggests that the binding conformations are similar but the effects of the binding interactions are different in POPC SUVs and LUVs. For compound **3**, the two spectra are more similar in shape however the spectrum in the presence of the SUVs is much more intense. This data suggests that the binding conformations are similar but the effects of the binding interactions are different in POPC SUVs and LUVs. For compound **2**, the same trend observed for compound **3**, is repeated. For compound **1**, the shapes and the intensities of the spectra are different, with the spectrum in the presence of the POPC SUV being the more intense. This data suggests that both the conformations adopted and the effect of the binding interactions on binding to POPC LUVs and SUVs are different. This implies that the curvature or other structural features of the SUV plays a major role in defining the binding of compound **1**, which is logical since compound **1**, contains the shortest Spacer #2. For compound **5**, both the shapes and the intensities of the spectra are different again suggesting that the conformations adopted and the effects of the binding interactions are different on binding to POPC LUVs and SUVs. This difference is most likely due to the effect of the curvature or other structural features of the SUV on the delocalized charge of the side chain guanidinium group versus the hard positive charge of the side chain amine functionality.

3.2.4. 4:1 POPC/POPG LUVs

The CD spectra of 100 μM solutions of compounds **4**, **3**, **2**, **1** and **5** in the presence of 1.75 mM 4:1 POPC/POPG LUVs are given in Figure 9A. These CD spectra are different from the corresponding spectra in POPC LUVs, (Fig. 5A) thus indicating that these compounds adopt different conformations on binding to anionic and zwitterionic LUVs. This observation is critical from a therapeutic perspective. If these compounds are to be useful therapeutic agents they must interact with mammalian and bacterial cells via different mechanisms, one mechanism leading to lyses of the bacteria cell, the other hopefully only surface interactions with mammalian red blood cells. The shapes of the CD spectra of these five compounds in the presence of 4:1 POPC/POPG LUVs are similar in shape, however they exhibit different intensities. There is no correlation between spectral intensity and Spacer #2 length. It should also be noted that the CD spectra observed in the presence of SDS micelles are different from the CD spectra observed in the presence of 4:1 POPC/POPG LUVs indicating that these AMPs interact with LUVs via more complex interactions than just surface binding.

The same titration experiments previously mentioned for POPC were also performed for 4:1 POPC/POPG LUVs. A peptide concentration of 200 μM was used for compounds **4**, **3**, **1** and **2** and a concentration of 100 μM was used for compound **5**. The concentration

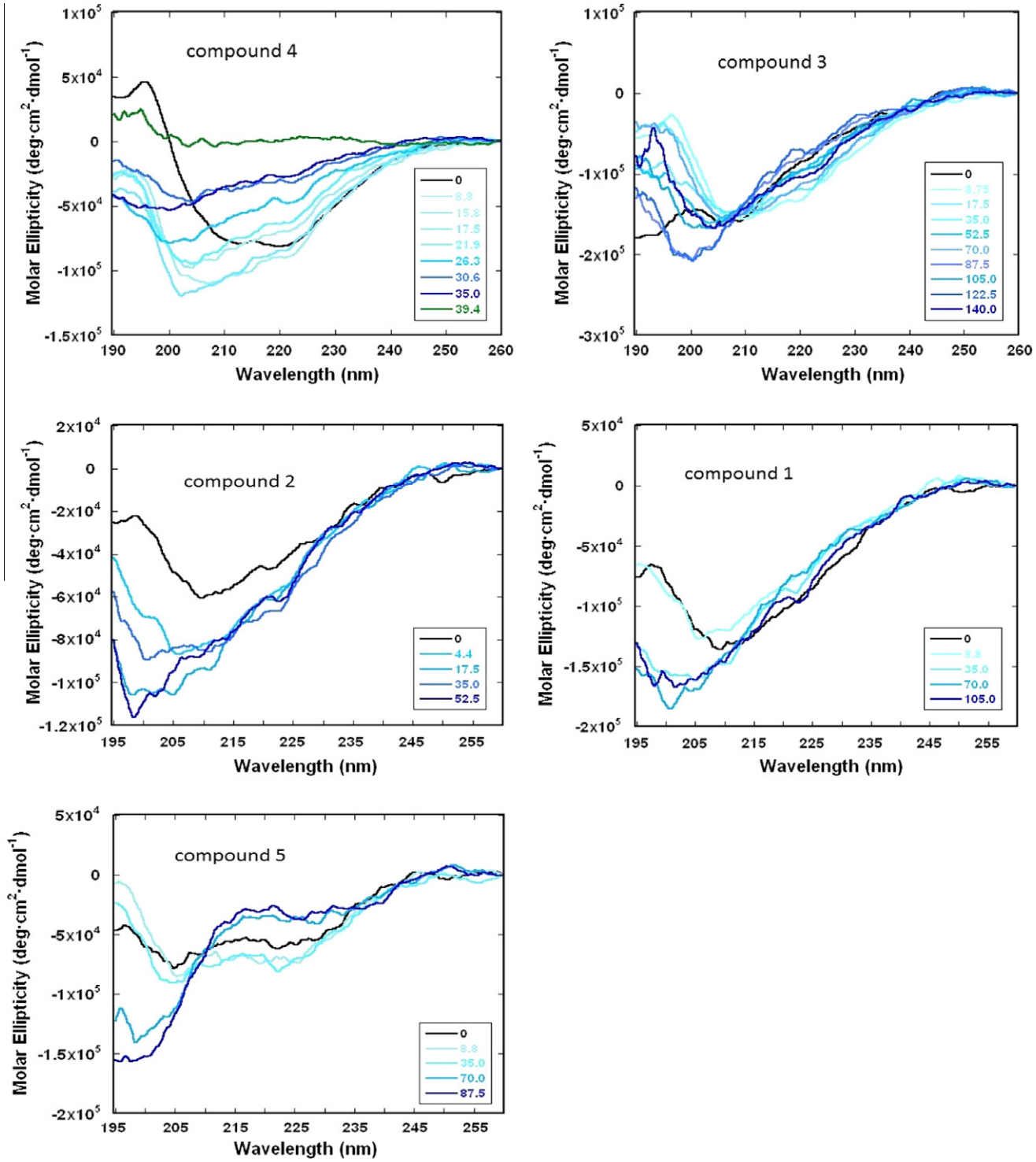

Figure 7. Far-UV circular dichroism spectra of compounds **4** (top left), **3** (top right), **2** (middle left), **1** (middle right) and **5** (bottom) with increasing concentration of POPC LUVs (0.8 – 12 mM). Color coding as the lipid to peptide ratio increases starting with a light blue color the corresponding spectra are shown in increasingly darkening blue color.

for the 4:1 POPC/POPG LUVs varied from 0.8 to 11 mM. The spectra for compounds **4**, **3**, **2**, **1** and **5** can be seen in Figure 10. For all of the compounds except compound **1**, the intensity of the CD signal decreases with increasing LUVs concentration, until a 'critical ratio'[72,73] is reached, which is unique to each peptide. For compound **4**, this ratio as previously reported[15] is approximately 39, for compound **3**, it is 36, for compound **2**, it is 22 and for compound **5**, it is approximately 52. Once this 'critical ratio' is reached the CD signal intensity starts to increase with increasing LUVs concentration. These titrations in all cases (except compound **1**) gave three groupings of CD spectra. The first group yields decreasing spectral intensity with increasing LUV concentration. The second group is limited to one transition point where the observed CD spectrum exhibits its minimum intensity. In the third and final grouping the spectral intensity increases with increasing LUV concentration. This observation is consistent with the proposal of Huang and

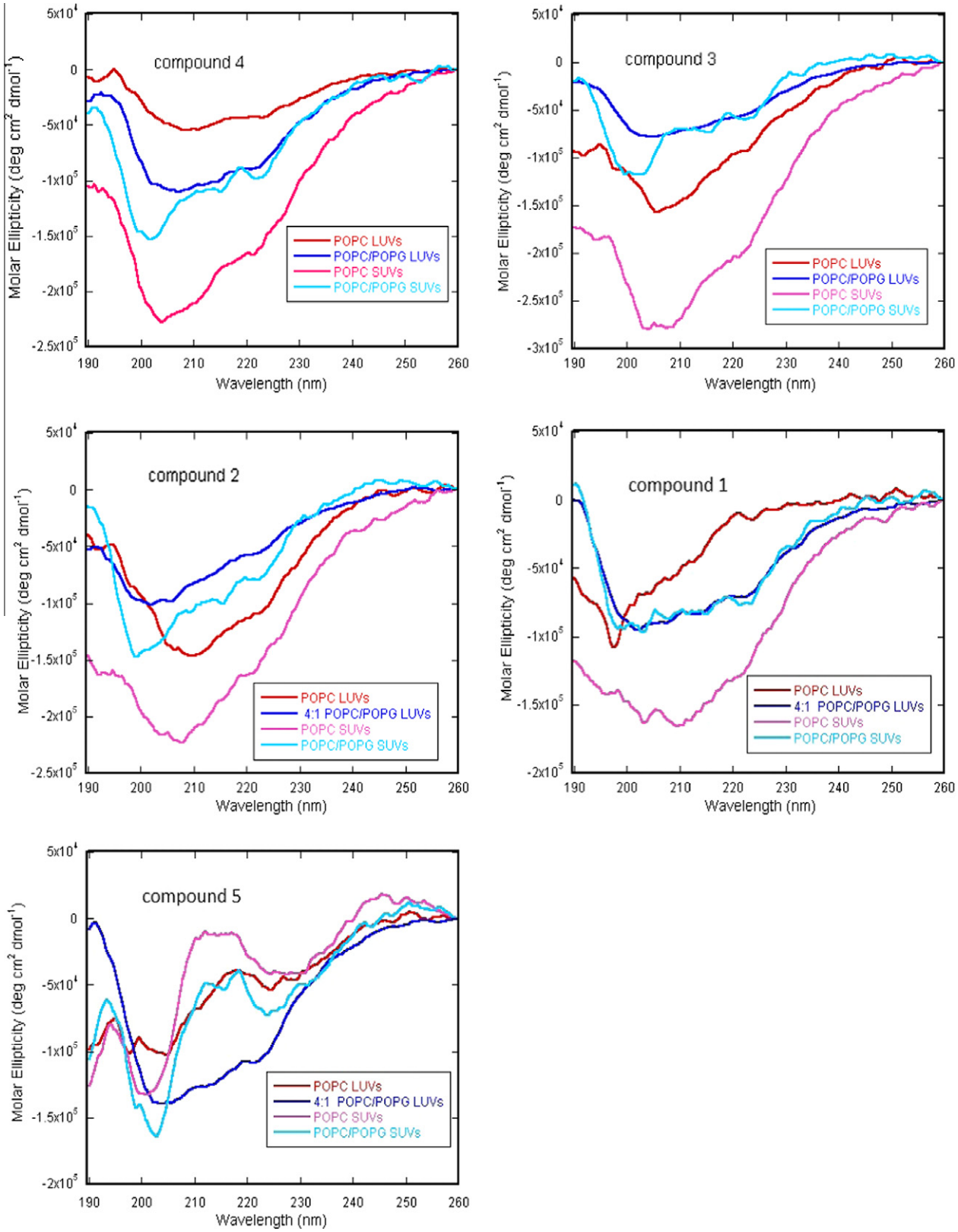

Figure 8. Comparison of the CD spectra in the presence of 1.75 mM POPC LUVs, 1.75 mM POPC/POPG LUVs, 1.75 mM POPC SUVs, and 1.75 mM 4:1 POPC/POPG SUVs, of compounds **4** (top left), **3** (top right), **2** (middle left), **1** (middle right) and **5** (bottom).

co-workers[72] that membrane thinning is a dominant factor in membrane distribution and pore formation. During the process of membrane distribution and pore formation, compounds initially bind to the surface of the LUV and cause a thinning of the LUV.[72,73] LUV thinning continues until a 'threshold peptide/LUV ratio' is reached. After this 'threshold ratio' no additional LUV

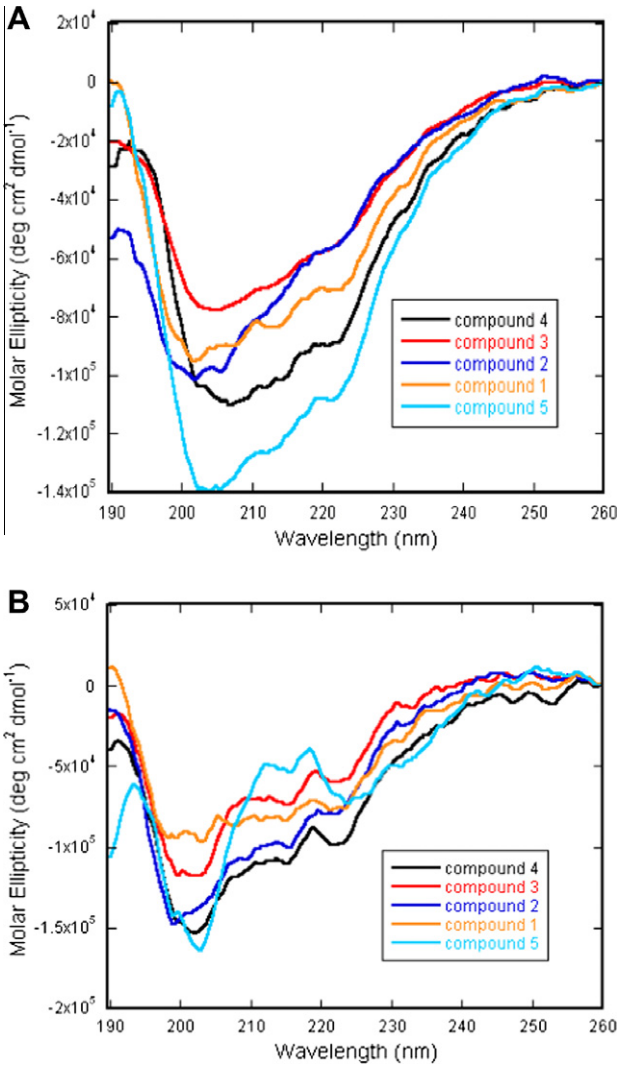

Figure 9. Far-UV circular dichroism spectra of 100 μM solutions of compounds **4**, **3**, **2**, **1** and **5** in the presence of (A) 1.75 mM 4:1 POPC/POPG LUVs; (B) 1.75 mM 4:1 POPC/POPG SUVs.

thinning occurs and the compounds now insert into the LUVs' hydrophobic core to form pores.[72,73] Huang and co-workers report that this "threshold ratio" depends to some extent on the particular compound and LUV involved in the binding process(the "threshold ratio" generally is close to 1:50).[72,73] The CD spectra of compound **1** in the presence of increasing concentrations of 4:1 POPC/POPG LUVs does not exhibits the concentration dependent behavior observed for the other four AMPs. In fact compound **1** exhibits the same behavior in 4:1 POPC/POPG LUVs as it did in POPC LUVs. This data clearly indicates that compound **1** with the shortest Spacer #2 interacts with 4:1 POPC/POPG LUVs via a different mechanism from the other four compounds.

3.2.5. 4:1 POPC/POPG SUVs

Comparing Figure 9A with B it appears that CD spectra of these compounds in the presence of 4:1 POPC/POPG SUVs and LUVs are dissimilar. The shapes and the intensities of the CD spectra of these five compounds on binding to 4:1 POPC/POPG SUVs are relatively similar, however there is no correlation to the λ_{min} at approximately 205 nm with the length of Spacer #2. The differences in the CD spectra for these compounds bound to 4:1 POPC/POPG LUVs and SUVs, are further illustrated in Fig. 8. For compound **4**, the CD spectrum in SUVs exhibits a different shape, but similar intensity to the CD spectrum observed in LUVs. This data suggests that compound **4**, adopts different conformations with the effect of the binding interactions being similar on binding to SUVs as compared to LUVs. For compound **3** the CD spectra exhibits the same trends as observed for compound **4**. For compound **2**, CD spectra in both SUVs and LUVs are more similar in shape, however, the spectrum in the presence of 4:1 POPC/POPG SUVs is more intense. This data suggests that in the presence of 4:1 POPC/POPG LUVs and SUVs, compound **2** adopts a similar conformation on binding but the effect of the binding interactions are different between the two systems. For compound **1**, the shapes and the intensities for CD spectra in the presence of 4:1 POPC/POPG LUVs and SUVs are almost identical suggesting that in both environments compound **1**, adopts the same binding conformation and experiences similar effects from the binding interactions. For compound **5**, both the shapes and the intensities of the spectra are very different again suggesting that the conformations adopted and the effect of the binding interactions are very different on binding to 4:1 POPC/POPG LUVs and SUVs. This difference is most likely due to the effect of the curvature or other structural differences of the SUV on the delocalized charge of the side chain guanidinium group versus the hard positive charge of the side chain amine functional group.

3.3. ITC studies

The application of isothermal titration calorimetry to study peptide LUV interactions is well documented in the literature.[42,43,45,53] Wieprecht and co-workers proposed that the binding of a peptide to a LUV is dependent on the global structural physicochemical properties such as the overall charge, hydrophobicity, and amphipathicity and not solely on the primary amino acid sequence of the peptide.[47]

3.3.1. POPC LUVs

As previously reported[15] titration of POPC LUVs into compound **4**, resulted in an endothermic reaction. Previous ITC studies on other compounds[76] have noted that an endothermic phase can be attributed to a combination of electrostatic interactions between the peptide and the membrane surface, disruption of polar head groups accompanied by reorganization of lipids on the surface of the membrane, disruption of the solvation spheres around the peptide and the membrane surface as well as other less understood phenomena.[76] The titration of POPC LUVs into compounds **3**, **2**, **1** and **5** also resulted in endothermic reactions as well (Fig. 11). Compound **5** transitions from an endothermic phase to an exothermic phase this indicates a different mechanism of binding to POPC LUVs as compared to the other four compounds. This observation is supported by the calcein leakage data discussed previously. As the length of Spacer #2 gets shorter, the molar ratio (lipid to peptide) for the interaction to reach completion remains constant except for the shortest side chain (compound **4**, the ratio is approximately 120, for compound **3**, it is 130, for compound **2**, it is 130, and for compound **5**, it is 150, however for compound **1**, it is reduced to 55) suggesting relatively weak binding to POPC LUVs for all of the analogs except for compound **1**, where Spacer #2 is a Dpr residue.

Binding isotherms for these peptides were developed. The value c_m for each compound was plotted against X_b, yielding a binding constant K for each compound. As seen in Table 3, the thermodynamic values for these compounds are similar and no clear correlation with Spacer #2 length can be made. To obtain enthalpy (ΔH) values for the binding interaction, single injection ITC experiments were conducted (Table 4).[44,77,78] These ΔHs should not be confused with ΔH^0, the enthalpy of the entire reaction, as they focus on the one extreme of the isotherm, binding. By titrating minimal (0.2 mM) compound into excess POPC LUVs (15 mM), it is

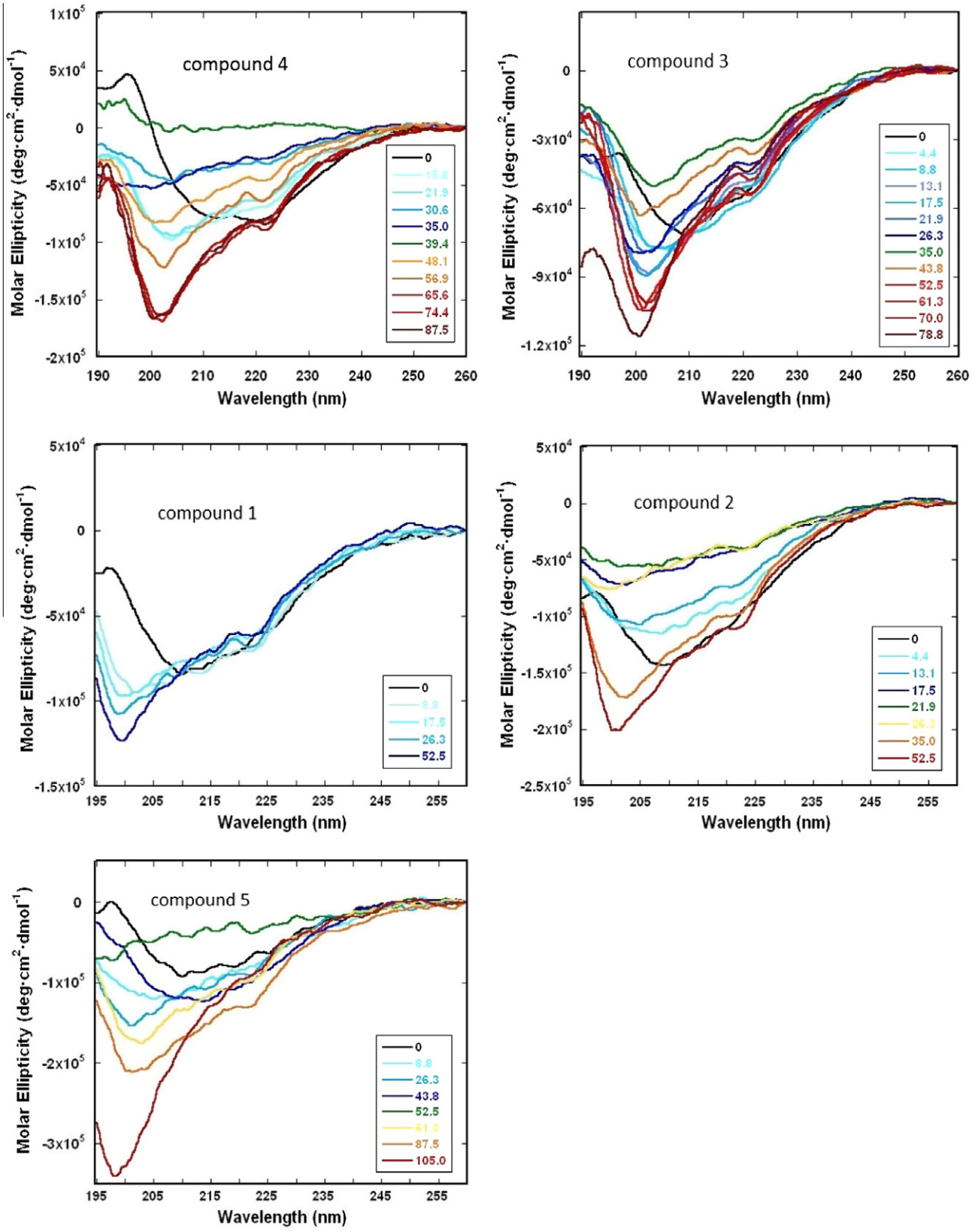

Figure 10. Representative CD spectra of compounds **4** (top left), **3** (top right), **2** (middle right), **1** (middle left) and **5** (bottom) with increasing concentration of 4:1 POPC/POPG LUVs (0.8–11 mM). Color coding as the lipid to peptide ratio increases starting with a light blue color the corresponding spectra are shown in increasingly darkening blue color with decreasing spectral intensity. Until a lipid to peptide ratio is reached where the CD spectrum reaches its minimum intensity (spectrum shown in green, this spectrum represents the 'critical point'). Increasing the lipid to peptide ratio after this point causes the spectral intensity to increase and the spectra are shown in darkening shades of red.

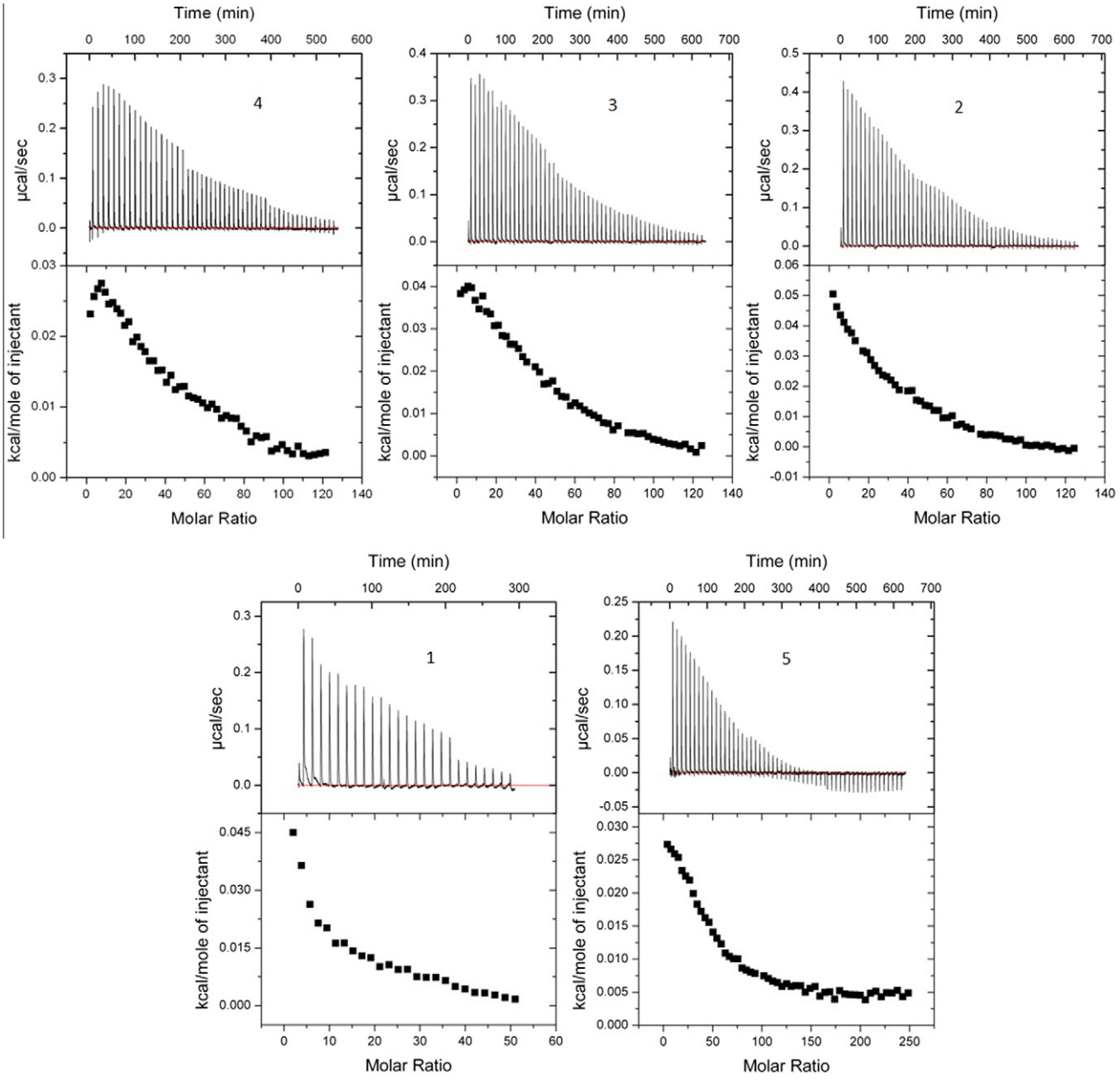

Figure 11. ITC data for the titration of 35 mM POPC liposomes into 0.2 mM of compounds **4** (top left), **3** (top middle), **2** (top left), **1** (bottom right) and **5** (bottom left). The experiment was run in 40 mM sodium phosphate buffer, pH 6.8, at a temperature of 25 °C and a stirring speed of 220 rpm.

Table 3
Thermodynamic parameters of binding of peptides to POPC vesicles at 25 °C

Compound	ΔH[a] (kcal/mol)	K[b] (M^{-1})	G[c] (kcal/mol)	ΔS[d] (cal/mol K)
4	0.67	211.0	−5.54	20.84
3	1.26	190.68	−5.48	22.64
2	1.17	239.77	−5.62	22.77
1	0.15	569.50	−6.13	21.09
5	0.77	479.39	−6.03	22.81

[a] ΔH values are directly measured binding enthalpies and calculated using Eq. 2.
[b] Binding constants were generated from the lipid-into-peptide titration using as described in the text.
[c] Free energies were calculated using Eq. 3.
[d] Entropy was calculated using Eq. 4.

Table 4
Single injection ITC data

Compound #	Compound into 4:1 POPC/POPG	Compound into POPC
4	−1.00 ± 0.04	2.10 ± 0.04
3	−2.75 ± 0.18	1.23 ± 0.03
2	−1.85 ± 0.12	−1.21 ± 0.07
1	−1.86 ± 0.05	−3.02 ± 0.14
5	−2.84 ± 0.19	−1.66 ± 0.09

possible to isolate the heat associated with the initial binding that occurs between the peptide and membrane surface. For compound **4** the binding process results in a ΔH of +2.10 kcal/mol as Spacer #2 gets shorter, ΔH transitions to a value of −3.02 kcal/mol for compound **1**. As the length of Spacer #2 decreases the binding with POPC LUVs goes from an enthalpically disfavored process to an enthalpically favored process. The fact that ΔH starts out positive, and not negative as observed in most 'binding' events, is due to several different processes. These processes include, but are not limited to, the removal of water molecules from the surfaces of

the membrane and peptide, movement of polar lipid head groups upon interaction with the peptide, disruption of lipid–lipid interactions as the hydrophobic side chain inserts into the bilayer to anchor the peptide and any repulsive interactions between the positive side chains and negative polar head groups.[56,76,79,80] The processes contribute to a $+\Delta H$, and thus counteract the $-\Delta H$ of binding to give an overall endothermic reaction.[56,76,79,80] The change in ΔH from positive to negative as a function of the length of Spacer #2 indicates that the relative contributions of the processes associated with binding are changing as a function of Spacer # 2 length.

3.3.2. 4:1 POPC/POPG LUVs

The titration of these compounds with 4:1 POPC/POPG LUVs resulted in an endothermic reaction followed by a transition to an exothermic reaction. The appearance of the thermograms for compounds **3**, **2** and **5** were very similar to that of compound **4** (Fig. 12).[15] As Spacer #2, gets shorter, the molar ratio (LUV to peptide) for the interaction to reach completion remains constant except for the shortest side chain (compound **4**, the ratio is approximately 30, for compound **3**, it is 28, for compound **2**, it is 20 and for compound **5**, it is 30), suggesting relatively strong binding by these peptides to 4:1 POPC/POPG LUVs. However, compound **1**, with the shortest Spacer #2, exhibited the weakest and shortest duration endothermic component followed by a rapid transition into a very strong exothermic phase that reached completion at a peptide to LUV ratio of 55. Due to the complexity of the thermograms we were unable to fit thermodynamic data to an existing model. Andrushchenko and co-workers also reported similar thermograms that transition from an endothermic phase to an exothermic phase for the binding of the tryptophan-rich cathelicidin antimicrobial peptides tritrpo4 and tritrpo6 with 7:3 POPE/POPG

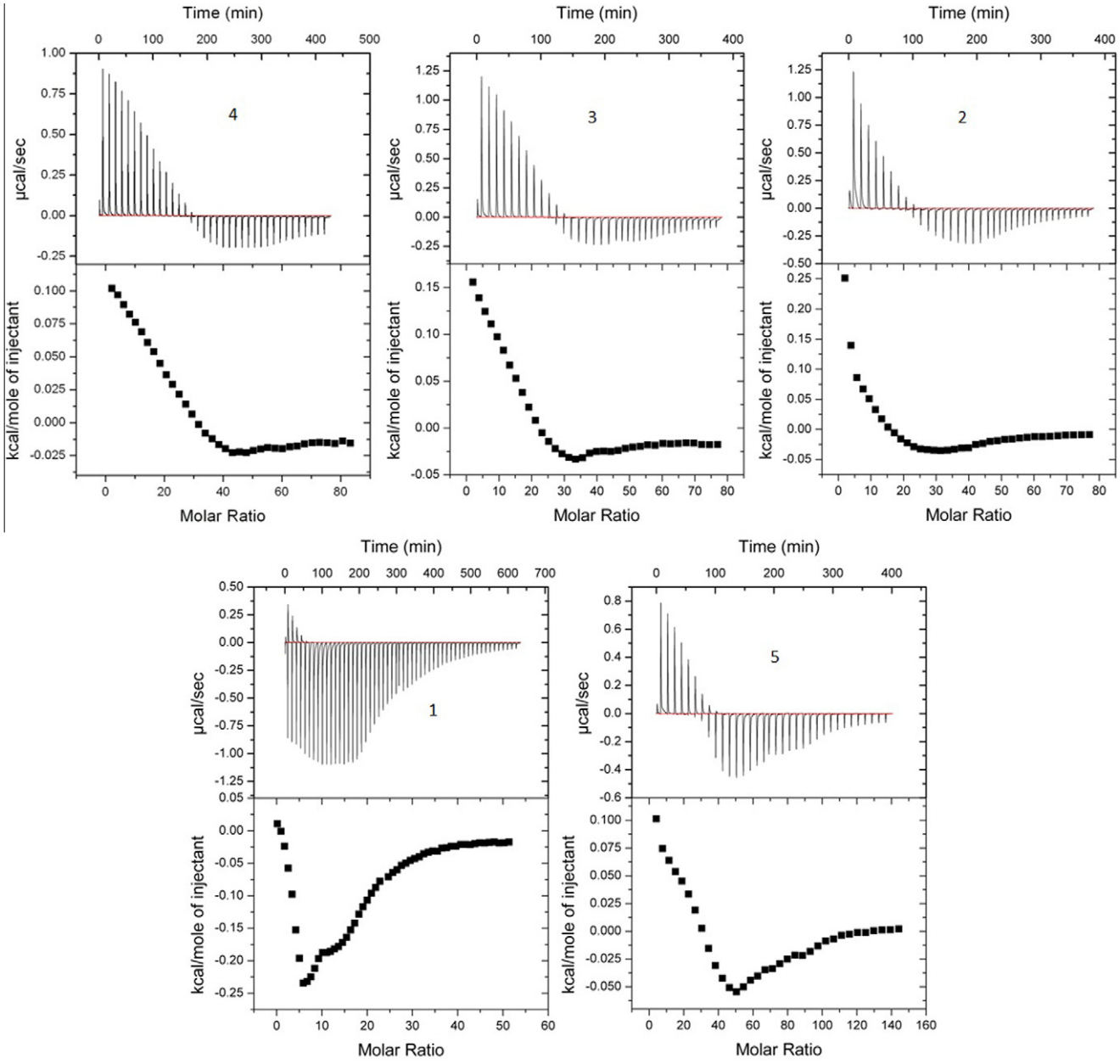

Figure 12. ITC data for the titration of 35 mM 4:1 POPC/POPG liposomes into 0.2 mM of compounds **4** (top left), **3** (top middle), **2** (top left), **1** (bottom right) and **5** (bottom left). The experiment was run in 40 mM sodium phosphate buffer, pH 6.8, at a temperature of 25 °C and a stirring speed of 220 rpm.

LUVs.[64] They ascribed the observation of both endothermic and exothermic phases to various processes occurring concurrently with binding including pore formation,[47] changes in the lipid phase properties[80] or peptide aggregation.[64] They concluded that the superimposition of the binding process onto the other concurrent process makes it impossible to derive binding parameters for these types of thermograms.[64] To obtain enthalpy (ΔH) values for the binding interactions, single injection ITC experiments were conducted (Table 4).[44,77,78] By titrating minimal (0.2 mM) compounds into excess 4:1 POPC/POPGLUVs (15 mM), it is possible to isolate the heat associated with the initial binding that occurs between the peptide and membrane surface. However unlike the case with POPC LUVs there is no correlation of ΔH with Spacer # 2 length. However the most active compounds **3** and **5** did exhibit the largest ΔH values of −2.75 and −2.84 kcal/mol, respectively.

Additional analysis of this data is required before a full explanation can be developed. However, clearly compounds **3**, **1**, **2** and **5** interact thermodynamically via a different mechanism(s) with POPC and 4:1 POPC/POPG LUVs. Also compound **1** interacts with 4:1 POPC/POPG LUVs via a different mechanism than compounds **3**, **2** and **5**.

4. Conclusion

It is very difficult to correlate the observed spectroscopic and thermodynamic data of these AMPs in the presence of membrane model systems to their biological activity. What is clear is that the length of Spacer #2 plays a major role in defining how these compounds interact with membranes and thus their resulting biological activity. The following has been demonstrated: (1) These peptides interact with anionic and zwitterion membrane models via different mechanisms. From a therapeutic perspective, it is a critical observation that indicates it may be possible to obtain selectivity for bacterial cells versus mammalian cells. (2) Within a class of membrane model, i.e. POPC LUVs, Spacer #2, defines how these peptides interact with that specific model. (3) The curvature and other structural properties of SUVs affects the conformations and binding affinity of these peptides differently than the structural properties of LUVs. (4) The properties of Spacer #2 (flexibility, charge density, hydrophobicity) seem to define organism selectivity and potency. (5) The hydrophobicity of the Spacer #2, seems to plays a role in defining antibacterial activity against selected strains of Gram negative bacteria.

Clearly, the properties of Spacer #2, play a critical role in making these AMPs 'responsive' to changes in the chemical composition and properties of membrane model systems. This 'responsiveness' to changes in chemical composition and properties of membranes is the most likely explanation to the observed organism selectivity and potency of these compounds.

Acknowledgments

The authors would like to acknowledge funding from the Bacterial Therapeutics Program 2.1 of the Defense Threat Reduction Agency. Contract # W81XWH-08-2-0095. The authors would also like to acknowledge funding from the North Carolina Biotechnology Center Grant Number 2006-FRG-1015 and from East Carolina University.

References

1. Bush, K. *ASM News* **2004**, *70*, 282.
2. Hartl, G., World Health Organization, 2000.
3. Shlaes, D. M.; Projan, S. J.; Edwards, J. E. *ASM News* **2004**, *70*, 275.
4. Huang, Y.; Huang, J.; Chen, Y. *Protein Cell* **2010**, *1*, 143.
5. Godballe, T.; Nilsson, L. L.; Petersen, P. D.; Jenssen, H. *Chem. Biol. Drug Des.* **2011**, *77*, 107.
6. Song, J. *Int. J. Antimicrob. Agents* **2008**, *32*, S207.
7. Findlay, B.; Zhanel, G. G.; Schweizer, F. *Antimicrob. Agents Chemother.* **2010**, *54*, 4049.
8. Kamysz, W. *Nuclear Med. Rev.* **2005**, *8*, 78.
9. Zhang, L.; Harris, S. C.; Falla, T. J. *Therapeutic Application of Innate Immunity Peptides*; Horizon Bioscience: San Diego, 2005.
10. Toke, O. *Biopolymers* **2005**, *80*, 717.
11. Ryge, T. S.; Frimodt-Moller, N.; Hansen, P. R. *Chemotherapy* **2008**, *54*, 152.
12. Hicks, R. P.; Bhonsle, J. B.; Venugopal, D.; Koser, B. W.; Magill, A. J. *J. Med. Chem.* **2007**, *50*, 3026.
13. Bhonsle, J. B.; Venugopal, D.; Huddler, D. P.; Magill, A. J.; Hicks, R. P. *J. Med. Chem.* **2007**, *50*, 6545.
14. Venugopal, D.; Klapper, D.; Srouji, A.; Bhonsle, J. B.; Borschel, R.; Mueller, A.; Russell, A. L.; Williams, B. C.; Hicks, R. P. *Bioorg. Med. Chem.* **2010**, *18*, 5137.
15. Russell, A. L.; Kennedy, A. M.; Spuches, A.; Venugopal, D.; Bhonsle, J. B.; Hicks, R. P. *Chem. Phys. Lipids* **2010**, *163*, 488.
16. Russell, A. L.; Kennedy, A. M.; Spuches, A. M.; Gibson, W. S.; Venugopal, D.; Klapper, D.; Srouji, A. H.; Bhonsle, J. B.; Hicks, R. P. *Chem. Phys. Lipids* **2011**, *164*, 740.
17. Russell, A. L.; Spuches, A. M.; Williams, B.; Venugopal, D.; Klapper, D.; Srouji, A. H.; Hicks, R. P. *Bioorg. Med. Chem.* **2011**, *19*, 7008.
18. Powers, J.-P. S.; Hancock, R. E. W. *Peptides* **2003**, *24*, 1681.
19. Glukhov, E.; Stark, M.; Burrows, L. L.; Deber, C. M. *J. Biol. Chem.* **2005**, *280*, 33960.
20. Giangaspero, A.; Sandri, L.; Tossi, A. *Eur. J. Biochem.* **2001**, *268*, 5589.
21. Dennison, S. R.; Wallace, J.; Harris, F.; Phoenix, D. A. *Protein Pept. Lett.* **2005**, *12*, 31.
22. Papo, N.; Shai, Y. *Biochemistry* **2003**, *42*, 9346.
23. Zhang, L.; Falla, T. J. *Curr. Opin. Investig. Drugs* **2009**, *10*, 164.
24. Yeaman, M. R.; Yount, N. Y. *Pharmacol. Rev.* **2003**, *55*, 27.
25. Leontiadou, H.; Mark, A. E.; Marrink, S. J. *J. Am. Chem. Soc.* **2006**, *128*, 12156.
26. Hancock, R. E. W.; Lehrer, R. *Trends Biotechnol.* **1998**, *16*, 82.
27. Goodman, M.; Shao, H. *Pure Appl. Chem.* **1996**, *66*, 1303.
28. Hendrickson, T. L.; de Crecy-Lagard, V.; Schimmel, P. *Annu. Rev. Biochem.* **2004**, *73*, 147.
29. Ma, J. S. *CHIMICA OGGI, Chemistry Today* 2003, 65.
30. Oh, J. E.; Lee, K. H. *Bioorg. Med. Chem.* **1999**, *7*, 2985.
31. Vasudev, P. G.; Chatterjee, S.; Shamala, N.; Balaram, P. *Chem. Rev.* **2010**. doi:10.1021/cr100100x.
32. Hicks, R. P.; Russell, A. L. In *Unnatural Amino Acids: Methods and Protocols*; Pollegioni, L., Servi, S., Eds.; Methods in Molecular Biology; Springer Science, 2012; Vol. 794, p 135.
33. Conlon, J. M.; Al-Ghaferi, N.; Abraham, B.; Leprince, J. *Methods* **2007**, *42*, 349.
34. Tossi, A.; Sandri, L.; Giangaspero, A. In *Proceeding of the 27th European Peptide Symposium Sorrento*; Benedetti, E., Pedone, C., Eds.; Edizioni Ziino: Napoli, Italy, 2002.
35. Lohner, K.; Prenner, E. J. *Biochim. Biophys. Acta* **1999**, *1462*, 141.
36. Grant, G. A. *Synthetic Peptides, A User's Guide*; Oxford University Press: New York, NY, 2002.
37. Benoiton, N. L. *Chemistry of Peptide Synthesis*; F1: Taylor and Francis (CRC Press): Boca-Raton, 2006.
38. Wieprecht, T.; Apostolov, O.; Seelig, J. *Biophys. Chem.* **2000**, *85*, 187.
39. Huang, C. H. *Biochemistry* **1969**, *8*, 344.
40. Ladokhin, A. S.; Vidal, M. F.; White, S. H. *J. Membr. Biol.* **2010**, *236*, 247.
41. Wei, S.-T. *J. Bacteriol.* **2006**, *188*, 328.
42. Hunter, H. N.; Jing, W.; Schibli, D. J.; Trinh, T.; Park, I. Y.; Kim, S. C.; Vogel, H. J. *Biochim. Biophys. Acta* **2005**, *1668*, 175.
43. Thomas, C. J.; Surolia, N.; Surolia, A. *J. Biol. Chem.* **2001**, *276*, 35701.
44. Wieprecht, T.; Apostolov, O.; Beyermann, M.; Seelig, J. *J. Mol. Biol.* **1999**, *294*, 785.
45. Wieprecht, T.; Beyermann, M.; Seelig, J. *Biophys. Chem.* **2002**, *96*, 191.
46. Wieprecht, T.; Seelig, J. In *Peptide-Lipid Interactions*; Simon, S. A., McIntosh, T. J., Eds.; Vol. Current Topics in Membranes; Academic Press: San Diego, 2002; p 32.
47. Wieprecht, T.; Apostolov, O.; Beyermann, M.; Seelig, J. *Biochemistry* **2000**, 442.
48. Wen, S. *J. Phys. Chem.* **2007**, *111*, 6280.
49. Kennedy, A.; Hmel, P. J.; Seelbaugh, J.; Quiles, J. Q.; Hicks, R. P.; Reid, T. J. *J. Liposome Res.* **2002**, *12*, 221.
50. Wieprecht, T.; Dathe, M.; Schumann, M.; Krause, E.; Beyermann, M.; Bienert, M. *Biochemistry* **1996**, 10844.
51. Dathe, M. *Biochemistry* **1996**, *35*, 12612.
52. Tamba, Y.; Yamazaki, M. *Biochemistry* **2005**, *44*, 15823.
53. Jing, W.; Hunter, H. N.; Hagel, J.; Vogel, H. J. *J. Pept. Res.* **2003**, *61*, 219.
54. Bringezu, F.; Wen, S.; Dante, S.; Hauss, T.; Majerowicz, M.; Waring, A. *Biochemistry* **2007**, *46*, 5678.
55. Abraham, T.; Lewis, R. N. A. H.; Hodges, R. S.; McElhaney, R. N. *Biochemistry* **2005**, *44*, 2103.
56. Seelig, J. *Biochim. Biophys. Acta* **1997**, *1331*, 103.
57. Seelig, J.; Nebel, S.; Ganz, P.; Bruns, C. *Biochemistry* **1993**, *32*, 9714.
58. Beschiaschvili, G.; Seelig, J. *Biochemistry* **1990**, *29*, 10995.
59. Beschiaschvili, G.; Seelig, J. *Biochemistry* **1990**, *29*, 52.
60. Benachir, T.; Lafleur, M. *Biochim. Biophys. Acta* **1995**, *1235*, 452.
61. Tachi, T.; Epand, R. F.; Epand, R. M. *Biochemistry* **2002**, *41*, 10723.
62. Mason, A. J.; Marquette, A.; Bechinger, B. *Biophys. J.* **2007**, *93*, 4289.
63. Seelig, J. *Biochim. Biophys. Acta* **2004**, *1666*, 40.

64. Andrushchenko, V. V.; Aarabi, M. H.; Nquyen, L. T.; Prenner, E. J.; Vogel, H. J. *Biochim. Biophys. Acta* **2008**, *1778*, 1004.
65. Seelig, J.; Ganz, P. *Biochemistry* **1991**, *30*, 9354.
66. Ladokhin, A. S.; Jayasinghe, S.; White, S. H. *Anal. Biochem.* **2000**, *285*, 235.
67. Medina, M. L.; Chapman, B. S.; Bolender, J. P.; Plesniak, L. A. *J. Pept. Sci.* **2002**, *59*, 149.
68. Glattli, A.; Daura, X.; Seebach, D.; van Gunsteren, W. F. *JACS* **2002**, *124*, 12972.
69. Ladokhin, A. S.; Selsted, M. E.; White, S. H. *Biochemistry* **1999**, *38*, 12313.
70. Berova, N.; Nakanishi, K.; Woody, R. W. *Circular Dichroism Principles and Applications*; Wiley-VCH: New York, 2000.
71. Watson, R. M.; Woody, R. W.; Lewis, R. V.; Bohle, D. S.; Andreotti, A. H.; Ray, B.; Miller, K. W. *Biochemistry* **2001**, *40*, 14037.
72. Chen, F.-Y.; Lee, M.-T.; Huang, H. W. *Biophys. J.* **2003**, *84*, 3751.
73. Almeida, P. F.; Pokorny, A. *Biochemistry* **2009**, *48*, 8083.
74. Ladokhin, A. S.; Jayasinghe, S.; White, S. H. *Anal. Biochem.* **2000**, *285*, 235.
75. Huang, H.; Schroeder, F.; Estes, M. K.; McPherson, T.; Ball, J. M. *Biochem. J.* **2004**, *380*, 723.
76. Abraham, T.; Lewis, R. N. A. H.; Hodges, R. S.; McElhaney, R. N. *Biochemistry* **2005**, *44*, 11279.
77. Normura, K.; Corzo, G. *Biochim. Biophys. Acta* **2006**, *1758*, 1475.
78. Wenk, M. R.; Seelig, J. *Biochemistry* **1998**, *37*, 3909.
79. Wieprecht, T.; Beyermann, M.; Seelig, J. *Biochemistry* **1999**, *38*, 10377.
80. Epand, R. M.; Segrest, J. P.; Anantharamaiah, G. M. *J. Biol. Chem.* **1990**, *265*, 20829.